

Evolution of the Turbulence Radial Wavenumber Spectrum near the L-H Transition in NSTX Ohmic Discharges

S. Kubota¹, C.E. Bush², R. Maingi², S. Zweben³, R.E. Bell³, N.A. Crocker¹, A. Diallo³, S.M. Kaye³, B.P. LeBlanc³, R.J. Maqueda⁴, J.-K. Park³, W.A. Peebles³, R. Raman⁵ and Y. Ren³

¹University of California at Los Angeles

²Oak Ridge National Laboratory, Oak Ridge, TN 37381

³Princeton Plasma Physics Laboratory, Princeton University, Princeton, NJ 08543

⁴Nova Photonics, Princeton, NJ 08540

⁵University of Washington, Seattle, WA 98195

Corresponding Author: skubota@ucla.edu

Abstract:

The turbulence characteristics near the L-H transition in NSTX Ohmic discharges are measured using the FMCW reflectometry and backscattering techniques. The unique capabilities of this diagnostic combination, i.e. sensitivity to the density profile as well as fluctuations up to $k_r \sim 22 \text{ cm}^{-1}$, are utilized to document the correlation between dynamics of the edge density gradient, turbulence correlation length, and the radial wavenumber spectrum, near the L-H transition in NSTX. During the L-mode phase, a broad band turbulence ($k_r \sim 2-10 \text{ cm}^{-1}$) extends over a significant portion of the edge-core from $R=120$ to 155 cm ($\rho=0.4-0.95$). At the L-H transition, turbulence is quenched across the measurable k_r range at the ETB location, where the radial correlation length also drops from ~ 1.5 to 0.5 cm . Close to the L-H transition, oscillations in the density gradient and edge turbulence quenching become highly correlated. These oscillations are also present in Ohmic discharges without an L-H transition, but are far less frequent. Similar behavior is also seen near the L-H transition in NB-heated discharges.

1 Introduction

The measurement of radially extended meso-scale structures such as zonal flows and streamers, as well as the underlying microinstabilities driving them, is critical for understanding turbulence-driven transport in plasma devices [1]. In particular, the shape and evolution of the radial wavenumber spectrum can indicate details of nonlinear spectral energy transfer [2], turbulence spreading [3], as well as transport barrier formation [4]. With respect to the L-H transition, significant progress has been made in terms of measurement capability and theory. Recent studies have concentrated on the interplay

between zonal flows and turbulence as an important component in the transition dynamic, however without a complete understanding of the physics, the power and conditions required for H-mode access on ITER remains an open questions. In the National Spherical Torus Experiment (NSTX) [5], zonal flows oscillations and associated quiet periods in the edge turbulence have been reported using gas-puff imaging (GPI) [6] in the L-mode phase of neutral beam-heated discharges, however the physical mechanism explaining the transition still remains elusive.

On NSTX, turbulence measurements are routinely made using a conventional set of microwave and millimeter-wave reflectometers (FMCW [7], fixed-frequency [8] and correlation [9]), which observe predominantly low- k fluctuations. The response of these diagnostics to modifications in the turbulence by flow shear or flow oscillations is therefore relatively poor. The frequency-modulated continuous-wave (FMCW) backscattering technique [10] retains the high time and spatial resolutions of the swept-frequency reflectometers ($\Delta t \gtrsim 10 \mu\text{s}$, $\Delta r \gtrsim 1 \text{ cm}$), while extending the spectral range up to $k_r \sim 22 \text{ cm}^{-1}$. This unique combination of capabilities in a single diagnostic allows fast dynamic events near the L-H transition to be monitored both at the microscopic (turbulence) and macroscopic (density profile) levels.

Initial measurements in NB-heated discharges revealed a strong correlation between the turbulence level and small changes in the density gradient in the vicinity of the ETB near the transition. The present article reports on measurements made near the L-H transition in Ohmic discharges (Shot 1417751, $I_p=800 \text{ kA}$, $B_T=3.5 \text{ kG}$, LSN, $\kappa \sim 1.9$, Deuterium). Ohmic plasmas in NSTX have peaked density profiles which provide good targets for the reflectometers. In addition, fast ion driven fluctuations as well as external momentum input and hot fueling from neutral beams are avoided, which can complicate

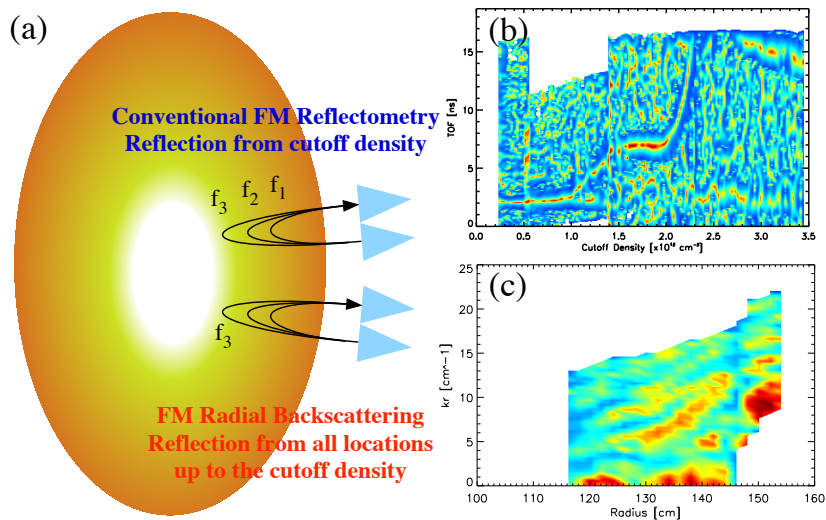


FIG. 1: (a) Conceptual drawing comparing traditional FMCW reflectometry and backscattering. (b) Radar backscatter image with axes $(\tau, n_c(f))$ from a single frequency sweep. (c) Backscatter image transformed to axes (r, k_r) and averaged over four sweeps.

both the physics interpretation and the turbulence measurements near the transition.

2 FMCW Backscattering Technique

The FMCW backscattering technique is similar to conventional 180° collective scattering, but with the following advantages: (i) a broad k_r response due to the swept frequency, and (ii) radial localization of the scattering volume determined from the time-of-flight. In typical FMCW systems, reflections can occur not only in the vicinity of the cutoff layer, but along the entire propagation path (see Fig. 1(a)). For a given frequency f and location r , the probed wavenumber k_r is derived from the Bragg rule: $k_r = 2k_0\mu(r, f)$, where k_0 is the vacuum wavenumber of the launched wave, $n_e(r)$ is the electron density, and $\mu(r, f)$ is the index of refraction. For the case of O-mode polarization, $\mu(r, f)$ is known wherever $n_e(r)$ is available. The time-of-flight at frequency f from a radius r_s can be written[11]

$$\tau(f, r_s) = \frac{2}{c} \int_{r_s}^{r_{\text{ref}}} \left[1 - \frac{f_{\text{pe}}^2(r)}{f^2} \right]^{-1/2} dr. \quad (1)$$

We note that Eq. 1 reverts to the time-of-flight used in profile inversion, when r_s is set to the cutoff radius $r_c(f)$. Figure 1(b) shows a radar image plot of the backscattered power as a function of the cutoff density $n_c(f) = m_e f^2 / 4\pi e^2$ and the time-of-flight τ . Using the Bragg rule, each pair of coordinates (τ, f) corresponds to a unique pair of coordinates (r_s, k_r) . Hence the contour plot in Fig. 1(b) can be transformed into the contour plot in Fig. 1(c) showing the power reflected as a function of k_r at each radial location. The true advantage of the technique comes from the fact that the same diagnostic data set can be used to generate $n_e(r)$ as well as the contours of the k_r spectrum. On NSTX, the swept-frequency range $f = 13\text{--}53$ GHz corresponds to the limit $k_r < 22$ cm $^{-1}$.

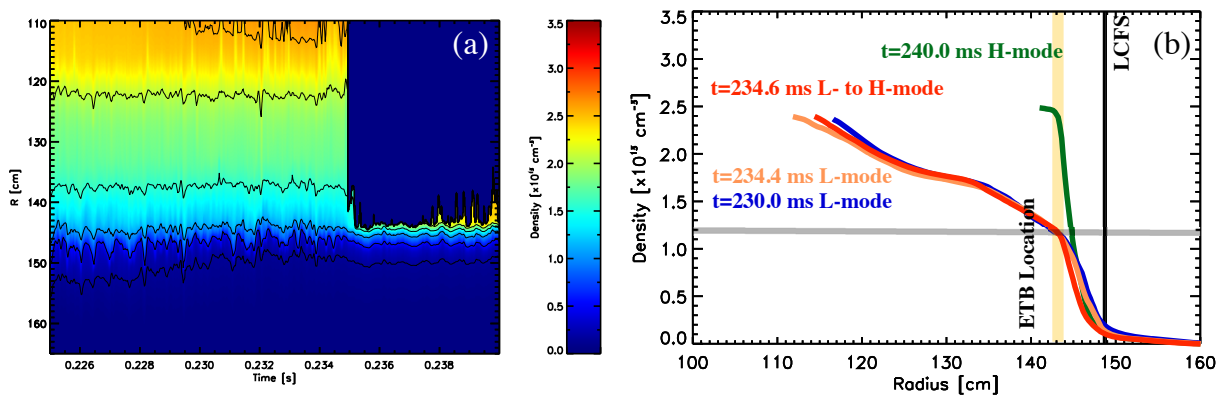


FIG. 2: (a) Contour plot of the density profile near the L-H transition, and (b) the density profile before and after the transition.

3 Turbulence Characteristics Near the L-H Transition

The temporal and spatial localization of the ETB is critical for observing the relevant dynamics leading to H-mode. Figure 2 shows the evolution of the electron density profile close to the L-H transition. In the L-mode phase, the edge density gradient undergoes intermittent steepening and relaxation. The final change in the profile at the transition itself occurs on the order of $\sim 100 \mu\text{s}$, and the subsequent development of an inverted edge density profile or “ears” prevents profile reconstruction further inwards. Figure 3(a) shows that the exact timing for the L-H transition ($t=234.64\pm 0.01 \text{ ms}$), as well as the radial location ($n_e=1.2\times 10^{13} \text{ cm}^{-3}$ corresponding to $r\approx 143-144 \text{ cm}$) of the ETB can be obtained by looking at the strength of the total reflected power from the FMCW reflectometers. The increase in reflected power after the L-H transition is caused by a combination of gradient steepening and the suppression of low- and intermediate- k turbulence, which has the effect of increasing the degree of specular reflection. This coincides temporally with the initial drop in the divertor D_α signal (see Fig. 3(b)), and spatially with the locations of the edge density “knee” in L-mode and the pedestal peak in H-mode (as shown in Fig. 2(b)).

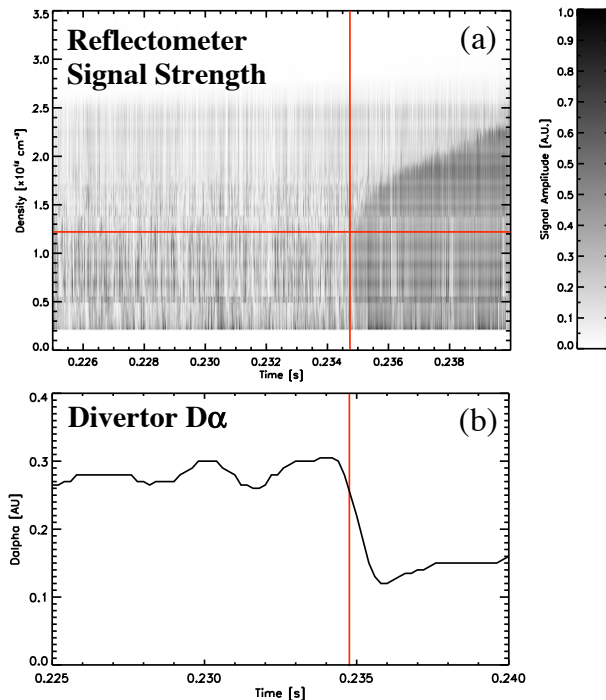


FIG. 3: (a) Evolution of the reflectometer signal strength as a function of the cutoff density, and (b) comparison with the divertor D_α signal. The red vertical and horizontal lines show the timing of the L-H transition and the density (or equivalently the position) where the ETB occurs. The sampling rate of the D_α signal is 5 kHz.

Further evidence of the highly localized nature of the ETB is displayed in Fig. 4, which shows both the k_r spectrum from backscattering (bottom-half), as well as the

radial correlation length L_{cr} (top-half) of low- k turbulence calculated from the FMCW reflectometer data using the technique outlined in Ref. [13]. Here L_{cr} is defined as the e -folding distance of the correlation coefficient function. Figure 4(a) shows that during the L-mode phase, L_{cr} displays little variation in time and ranges from ~ 2.5 cm at $R=135$ cm to ~ 1 cm at $R=145$ cm. These values are consistent with the typical observation [12] of $L_{\text{cr}} \sim \sqrt{L_n \rho_s} \sim 1-3$ cm for $L_n \sim 10-30$ cm and $\rho_s \sim 0.1-0.3$ cm in our case (here L_n is the density scale length and ρ_s is the ion sound gyro-radius). It is important to note that the L_{cr} measurements are limited to a time resolution of $\sim 300-400$ μs for good statistics. Figure 4(b) shows the k_r spectrum of the turbulence in the edge-core, which displays a broad spectral band ($k_r \sim 2-10$ cm^{-1}) that extends across a significant portion of the edge-core from $R=120$ to 155 cm ($\rho=0.45-0.95$). In contrast the region $\rho \lesssim 0.4$ is relatively turbulence free (only very low k_r fluctuations exist). The inner edge of the band seems to coincide with the kink in the density profile. It is interesting to note that the upper edge of the band (k_r -width) scales inversely with ρ_s ($k_r \rho_s \sim 2-3$), although a positive identification of these modes has yet to be made. These features are also seen in the L-mode portion of NB-heated H-mode discharges. Immediately after the L-H transition, L_{cr} drops from ~ 1.5 to ~ 0.5 cm at the ETB location, as shown in Fig. 4(c). Similarly, Fig. 4(d) shows only a local change in the k_r spectrum at the ETB location, where turbulence across the entire measurable spectral range ($k_r \sim 0-15$ cm^{-1}) is quenched.

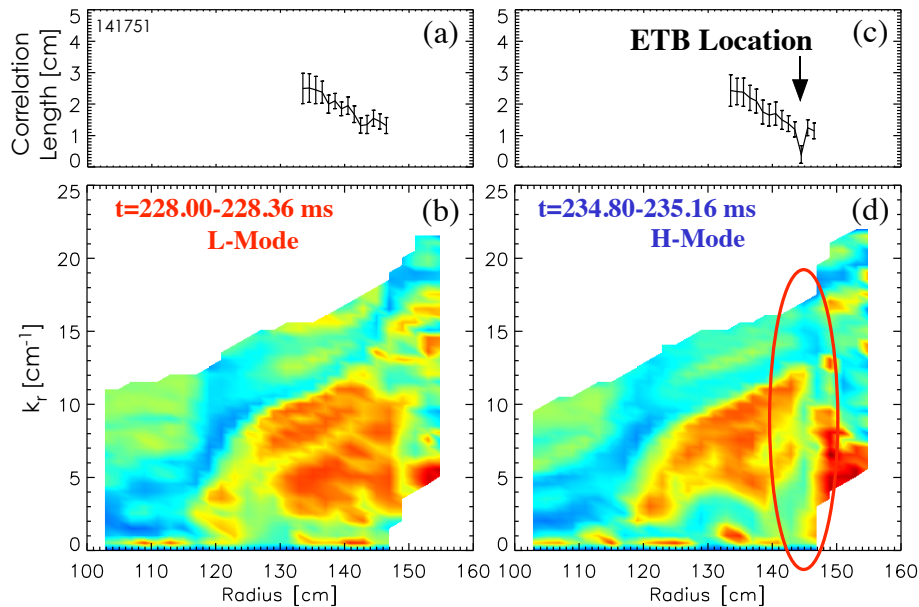


FIG. 4: The turbulence correlation length and k_r spectrum in L-mode (a) and (b), and H-mode (c) and (d). The red oval shows the region of the k_r spectrum where turbulence is quenched.

The L-mode phase leading up the H-mode transition shows a wealth of dynamics that is difficult to succinctly quantify. The k_r -spectrum and the edge density gradient at the ETB location exhibit both intermittent and cyclic oscillations, where the turbulence and edge

gradients are “L-” or “H-mode-like” before entering the final transition to H-mode. An example of these observations is shown in Fig. 5, which plots the variation of the density scale length L_n approaching the L-H transition, along with the total backscattered power (integral over k_r), at the ETB location. Here the troughs in L_n and the k_r spectral power represent “H-mode-like” states while the peaks represent “L-mode-like” states. In the “H-mode-like” state, these quantities intermittently (few tens to \sim hundred μ s duration) show the same trends that are seen shortly after the transition to H-mode. Closer to the L-H transition, the mean density gradient becomes steeper, while the oscillations (2–8 kHz) in the k_r spectral power become more frequent and increase in amplitude. In addition, the changes in L_n and the k_r spectral power show higher correlation.

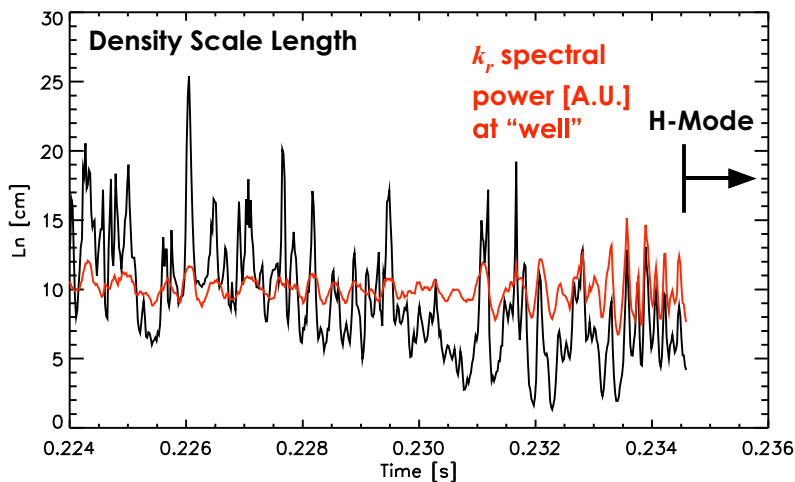


FIG. 5: Time evolution of the edge density scale length L_n and the k_r spectral power at the ETB location. The peaks and troughs in L_n and the spectral power correspond to the “L-” and “H-mode-like” states, respectively.

Finally, many discharges from the same data set include nearly identical shots where there is no apparent H-mode (or dithering) evident from the D_α or other signals. These discharges also exhibit intermittent “H-mode-like” states with steep edge gradients and lower k_r spectral power, but their occurrence is far less frequent.

4 Summary and Discussion

A new diagnostic technique (FMCW backscattering) has been used in NSTX Ohmic discharges to observe rapid changes in the edge turbulence k_r spectrum and the electron density profile near the L-H transition. The edge density at the ETB location exhibits oscillations between “L-” and “H-mode-like” states leading up to the L-H transition. Just after the L-H transition at the ETB location, the edge gradient steepens, the turbulence correlation length drops, and the power in the k_r spectrum is quenched. These results are similar to observations elsewhere of a very narrow \sim 1 cm transport barrier. During the

“H-mode-like” state in the L-mode phase, the density at the ETB location momentarily steepens and the k_r spectrum there is partially quenched.

The presence of oscillations between “L-” and “H-mode-like” states on NSTX seems to be ubiquitous for many discharges (Ohmic or NB-heated), whether there is ultimately a transition or not. While the dynamic behavior of and correlation between microscopic (k_r spectrum, L_{cr}) and macroscopic (edge density) length scales has been documented, questions such as the causal relationship between these observations and the reason for the localization to a specific radial location still remain. An important component of current zonal flow theories is the predator-prey relation between turbulence and zonal flows. The backscattering measurements show a broad band of turbulence in the edge-core extending spectrally into the intermediate- k_r range and radially outward beyond the location where the ETB forms. The modulation of this turbulence at the edge could be a sign of the predator-prey relation between turbulence and zonal-flows, which is an important component of recent L-H transition theories [14]. The “H-mode-like” state described here is qualitatively similar to the ~ 3 kHz “quiet periods” observed in NB-heated H-mode with GPI, where the edge turbulence was transiently suppressed leading up to the L-H transition [6]. Comparison of data from the microwave and GPI diagnostics for Ohmic H-mode discharges is currently under way.

FMCW reflectometry has been a standard diagnostic on many fusion plasma devices for at least two decades. FMCW backscattering simply reinterprets the data from FMCW reflectometry, hence this method could be applied to existing data sets going back many years. One open question is whether the properties of the spherical torus facilitate the measurements made on NSTX (e.g. magnetic geometry, overdense plasma, etc.). Finally, numerical studies using 1-D and 2-D GPU-based full-wave codes are under way to better estimate the spectral shape and amplitude of the turbulence from the backscattered signal.

5 Acknowledgements

Supported by U.S. DoE Grants DE-FG03-99-ER54527 and DE-AC02-09CH11466.

References

- [1] Fujisawa, A., et al., “Experimental studies of mesoscale structure and its interactions with microscale waves in plasma turbulence”, *Plasma Phys. Control. Fusion* 53, (2011) 124015.
- [2] Li, J. and Kishimoto, Y., “Wave-number spectral scaling of drift wave-zonal flow turbulence in gyrofluid simulations”, *Phys. Plasmas* 17, (2010) 072304.
- [3] Hahm, T.S., et al., “Turbulence spreading into the linearly stable zone and transport scaling”, *Plasma Phys. Control. Fusion* 46, (2004) A323.
- [4] Wang, W.X., et al., “Nonlocal properties of gyrokinetic turbulence and the role of $E \times B$ flow shear”, *Phys. Plasmas* 14, (2007) 072306.

- [5] Ono, M., et al., “Exploration of the spherical torus physics in the NSTX device”, Nucl. Fusion 40, (2000) 557.
- [6] Zweben, S.J., et al., “Quiet periods in edge turbulence preceding the L-H transition in the National Spherical Torus Experiment”, Phys. Plasmas 17, (2010) 102502.
- [7] Kubota, S., et al., “Ultrafast millimeter-wave frequency-modulated continuous-wave reflectometry for NSTX”, Rev. Sci. Instrum. 77, (2006) 10E926.
- [8] Crocker, N.A., “High spatial sampling global mode structure measurements via multichannel reflectometry in NSTX”, Plasma Phys. Control. Fusion 53, (2011) 105001.
- [9] Kubota, S., et al., “A Ka-band tunable direct-conversion correlation reflectometer for NSTX”, Rev. Sci. Instrum. 81, (2010) 10D917.
- [10] Kubota, S., et al., “Turbulence Characteristics Near the L-H Transition in NSTX Ohmic Discharges”, Presented at the 53rd Meeting of the APS Division of Plasma Physics, B04.00003 (2011).
- [11] Laviron, C. et al., “Reflectometry techniques for density profile measurements on fusion plasmas”, Plasma Phys. Control. Fusion 38, (1996) 905.
- [12] Doyle, E.J., et al., “Chapter 2: Plasma confinement and transport”, Nucl. Fusion 47, (2007) S18.
- [13] Kurzan, B., et al., “Measurement and scaling of the radial correlation lengths of turbulence at the plasma edge of ASDEX Upgrade”, Plasma Phys. Control. Fus. 42, 237.
- [14] Diamond, P.H., et al., “Zonal flows in plasma—a review”, Plasma Phys. Control. Fus. 47, (2005) R35.